Published by
NIGERIAN SOCIETY OF PHYSICAL SCIENCES
Available online @ https://journal.nsps.org.ng/index.php/jnsps

J. Nig. Soc. Phys. Sci. 4 (2022) 1050

Journal of the Nigerian Society of Physical Sciences

Structural, Optical and Electrical Properties of V_2O_5 Thin films by Spray Pyrolysis Method

A. Sherin Fathima, I. Kartharinal Punithavthy*, S. Johnson Jayakumar, A. Rajeshwari, A. Sindhya, A. Muthuvel

Department of Physics, T.B.M.L College (Affiliated to Bharathidasan University, Tiruchirapalli-620024), Porayar, Tamil Nadu-609307, India.

Abstract

Vanadium pentoxide (V_2O_5) and indium tin oxide (ITO) coated V_2O_5 thin films were prepared by hydrothermal technique. The influence of different molarity of V_2O_5 on the electrical properties of ITO-V_2O_5 films was investigated. The films were found to be polycrystalline and to belong to a V_2O_5 orthorhombic crystal system based on their X-ray diffraction (XRD) analysis. It was confirmed by Fourier transform infrared (FT-IR) spectrum that V_2O_5 functional groups formed a V-O bond. The optical band gaps were found to increases with increasing molarity in the range 2.18 – 2.89 eV. Scanning electron microscopy (SEM) analysis shows crumbled paper-like morphology in the sheet-like layer arrangement. The dielectric current (DC) electrical conductivity was studied as function of molarity which indicated the semiconducting nature. The morphological and structural studies show enhanced results for 4% sample which makes it a viable candidature for optical and electrical applications.

DOI:10.46481/jnsps.2022.1050

Keywords: V_2O_5 Thin films, Optical properties, Surface Morphology. Spray Pyrolysis, Electrical Properties.

Article History :
Received: 09 August 2022
Received in revised form: 14 October 2022
Accepted for publication: 17 October 2022
Published: 27 November 2022

Communicated by: K. Sakthipandi

1. Introduction

Transition metal oxides, especially vanadium compounds gain immense interest due to their special physical and chemical properties, making them technological useful for nanoscale device application [1-7]. A thin film of Transition metal oxides has been a wide platform of research in recent years due to their application in technological aspects. Thin films of V_2O_5 laid footprints in the sectors of gas sensors, solar cells, and batteries [8-9]. Vanadium combines with oxygen to form a variety of compounds with varying structural, optical, and chemical properties [10].

Various phases of vanadium oxides possess different properties based on their structural arrangement of atoms. The different phases like V_2O_5, V_2O_3, VO_2 and VO exhibit different properties. The different phases of vanadium oxides can be achieved through the modifications in the deposition process as well as due to the modification in the post-annealing line process. Although there exist several phases of Vanadium oxides, VO_2 and V_2O_5 have involved the consideration of the researchers, due to their thermochromic behaviour and electrochromic properties respectively. One of the thermodynamically stable phases of vanadium oxides is vanadium pentoxide thin films, which are also used in smart windows, optical filters, and surfaces with adjustable emittance for temperature control [11].

*Corresponding author tel. no: +91-9442422539
Email address: profpunithavthy@gmail.com, profpunithaphysics@gmail.com (I. Kartharinal Punithavthy)

In recent years, nanostructured vanadium oxide has been attracted considerable attention due to its organic and physical properties and their countless prospective for applications in catalysis [12] electrochromic devices [13] sensors [14] electrochemistry [15] photocatalytic activities [16] and spintronic devices [17]. V_2O_5, one of the more stable vanadium oxide phases, has a distinctive set of features and is one of the compositions of vanadium oxide that may be formed [18]. This substance is also employed as an intercalation chemical due to its two-dimensional layer structure. Since the discovery of the reversible electrochemical lithium-ion intercalation in V_2O_5 [19]. Due to its low cost, simplicity, synthesis, abundance and high energy density, vanadium pentoxide has received a lot of attention as a potential cathode material for rechargeable lithium-ion batteries. It is a typical embolism compound with a covered crystal structure that allows for the reversible intercalation and extraction of a wide range of atomic and molecular species. The energy storage and the charge/discharge rate are the most crucial factors for electrochemical pseudo capacitor applications. To obtain a high charge/discharge rate, a higher surface range and simple charge conveyance are needed [20]. V_2O_5 xerogel and aerogel, which together offer large surface range, have been travelled for numerous applications. Shenzhen Deng et al. recently reported electrochemical performance of vanadium oxide-based cathodes in aqueous zinc -ion batteries [21]. An ultrasound assisted synthesis of V_2O_5 nanoparticles for photocatalyst and antibacterial activity was reported by Karthik et al [22]. The hydrothermal method used by Muhammad Rafique et al. for degradation of RhB dye uses highly efficient and visible light driven Ni doped V_2O_5 photocatalysts [23]. Using Ar/O_2 gas mixtures, Benmoussa et al. successfully fabricated V_2O_5 thin films on indium tin oxide coated glasses [24]. In the present work, the deposition procedure of V_2O_5 films on the fused substrate was carried out first. Then the V_2O_5 thin film deposition on the ITO coated fused silica substrate was investigated. The prepared thin film was characterized by the XRD, FT-IR, SEM with EDAX and UV-visible spectroscopy. The electrical studied is measured with the V_2O_5 thin film deposited ITO coated fused silica substrate as a working film.

2. Experimental Procedure

The thermal evaporation of pure V_2O_5 Powder (purity 99.99 percent acquired from MERCK) from an electrically heated molybdenum boat held at 1823 K in a vacuum better than 8 x 10^{-6} Torr was used to creating thin coatings of V_2O_5 on ITO substrates. The experimental films were deposited using a Hind High Vacuum Coating machine. The final pressure was generated using a diffusion pump supported by a rotary pump. ITO substrate had been thoroughly cleaned and the appropriate covers were mounted on a copper holder that was set up on a tripod inside the bell jar. The distance between the source and substrate was set in cm. The glow discharge was started to further ionically clean the substrates in the vacuum chamber after achieving the ultimate vacuum of 5 x 10^{-6} Torr and the desired substrate temperature in the chamber and permitted to enter the system. The substance inside the boat evaporated when the power was applied, and the resulting vapours' reaction with the oxygen gas resulted in the deposition of a coating on the sub-

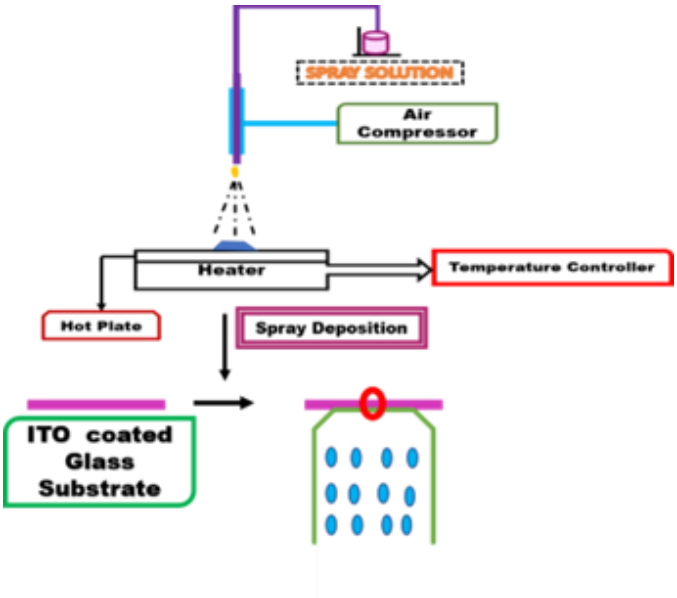

Figure 1: Flow chart for the synthesis of V_2O_5 thin films through spray pyrolysis method

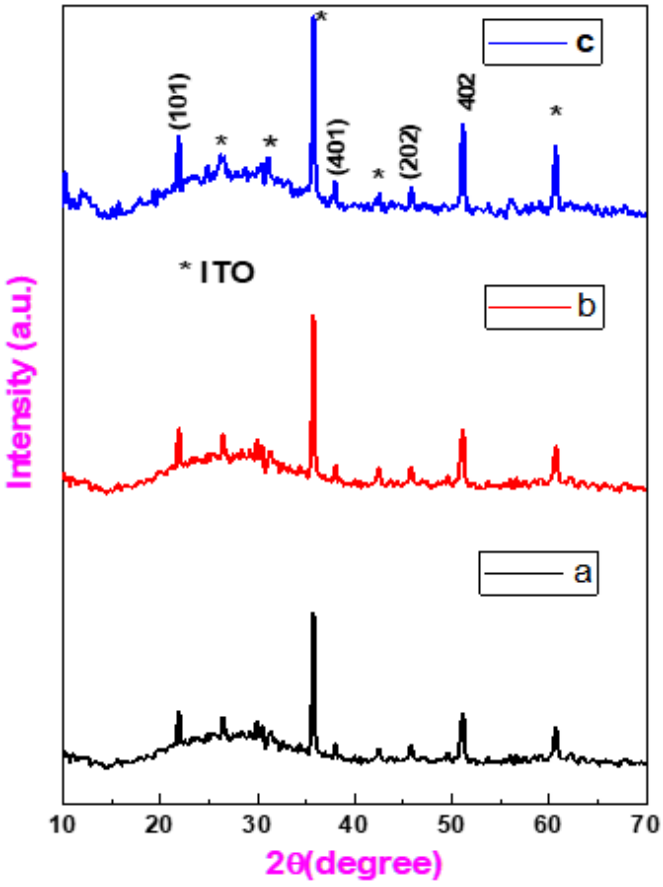

Figure 2: XRD patterns of (a) pure V_2O_5 (b-c) 2 and 4 % ITO coated V_2O_5 thin film

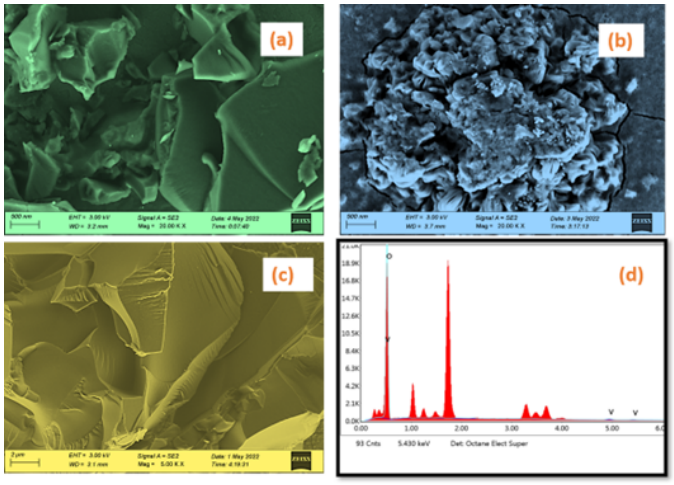

Figure 3: (a-c) SEM image (pure, 2 and 4 %) (d) EDAX of 2% molarities V_2O_5 thin films

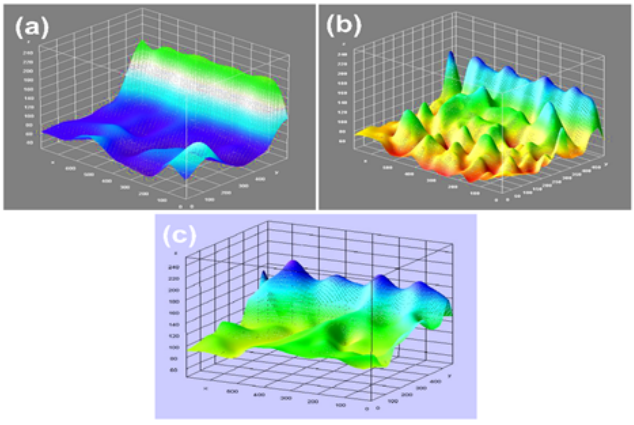

Figure 4: Surface Occupancy plots of thin films (a) pure V_2O_5, (b) V_2O_5 at 2% and (c) 4% molarities

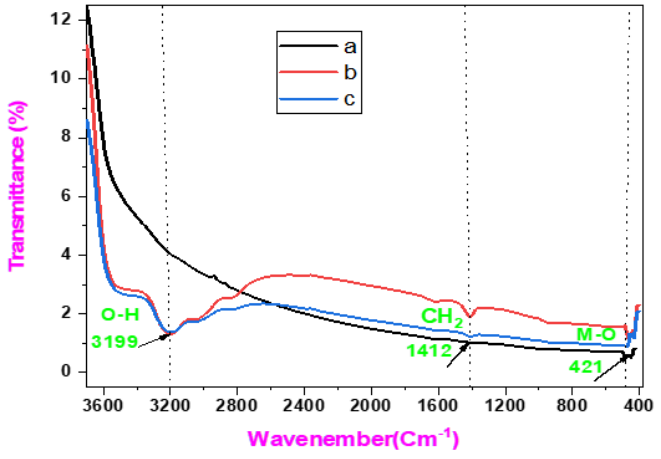

Figure 5: FTIR spectra of (a) pure V_2O_5 and (b-c) V_2O_5 with 2 and 4 % of molarities

strate. Using an optical pyrometer, the boat's temperature was measured during the deposition process. Following the maintenance of the substrates at the necessary deposition temperature, the molybdenum boat with the V_2O_5 powder was positioned. When the boat's temperature reached around 1823 K, the shutter covering the substrates was opened, and it remained open during the film deposition process. Fig 1 shows the chart for the synthesis of V_2O_5 thin films through spray pyrolysis method.

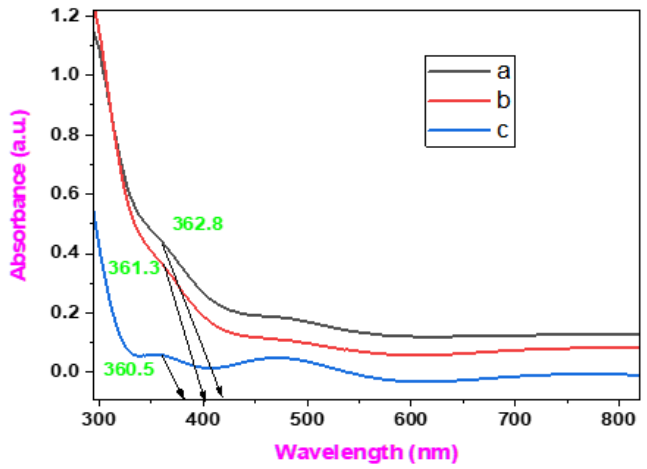

Figure 6: Optical absorption spectra of (a) Pure V_2O_5 thin films and (b-c) V_2O_5 thin films with 2 and 4 % of molarities

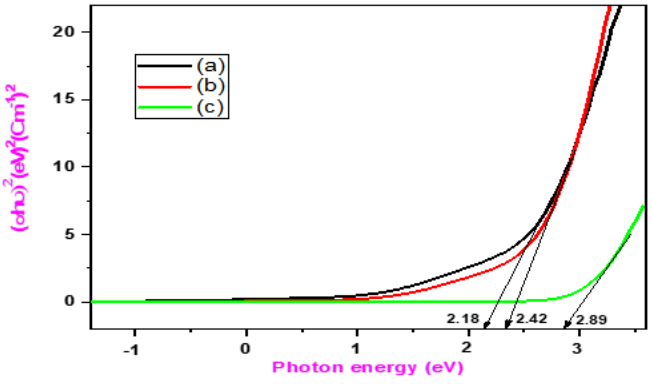

Figure 7: Band Gap energy of (a) Pure V_2O_5 thin films and (b-c) V_2O_5 thin films with 2 and 4 % of molarities

2.1. *Characterization*

In the present study, JASCO V-670 spectrophotometer was used to record optical spectra in the range of 300-800 nm. The crystalline phase structures of the products were examined and studied by X-ray diffractometer (Riakgu Mini Flexell) operated at a 40 KV and current 30 mA with Cukα (λ = 1.5406 Å). The interaction of functional groups in the synthesized nanoparticles was investigated using a Fourier transform infrared (FT-IR) spectrometer (BRUKER; RFS 27).

3. Results and Discussions

3.1. *XRD analysis*

The structural analysis of ITO-coated V_2O_5 thin films with two different molarities was carried out by XRD as shown in

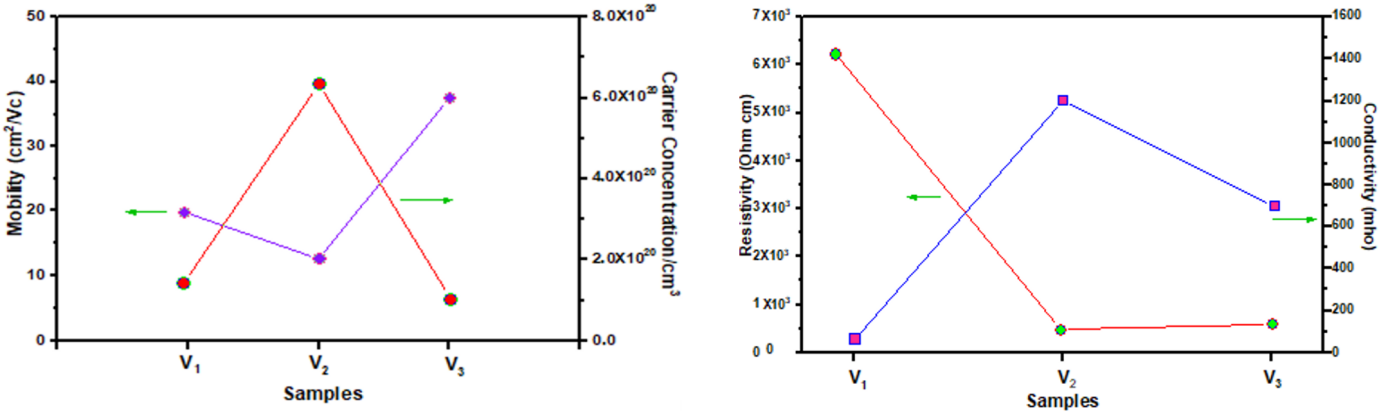

Figure 8: Electrical studies of pure and ITO (2 and 4%) coated V_2O_5 thin films

Table 1: Structural parameters of pure and ITO (2 and 4%) coated V_2O_5 thin film

S. No	Sample	Average crystallite size (D) X10^{-9}m	Average Dislocation density (δ) X10^{14}m^2	Average Microstrain (ε) X10^{-3}m
1	Pure	32.0	1.0087E^{+15}	0.00113
2	2%	29.5	1.14061^{E+15}	0.00122
3	4%	26.8	1.38471E^{+15}	0.00134

Table 2: Vibrational Assignments of Thin films (Pure V_2O_5 thin films, V_2O_5 with 2, 4% of Molarity)

S/N	Vibrational Assignments (cm^{-1})			Inference	**References**
	a	**b**	**c**		
1	421	421	421	Metal oxide stretching vibrations	[30]
2	1412	1412	1412	CH_2 - Bending Vibration of Carbon chain	[33]
3	3199	3199	3199	OH-Stretching Vibration	[32]

Table 3: Absorption and Band gap of pure and 2 and 4 % ITO coated V_2O_5 thin tilms

Composition	Absorbance	Bandgap (eV)
Pure V_2O_5	362.8	2.18
2%	361.3	2.42
4%	360.5	2.89

Fig 2. The diffraction peaks at 2θ = 21.50°, 30.71°, 38.41° and 45.7°correspond respectively to reflections from planes (101), (400), (211) and (002) indicating the formation of orthorhombic crystal structure of V_2O_5 which is agreed with the JCPDS card No.: JCPDS No.: 89-2482 [25]. Other peaks are due to the ITO coated glass substrate. As can be seen in all XRD spectra, the peaks are enhanced with different molarity as a sign of improved crystallinity (Fig 2).

Rathika *et al.* [26], synthesized V_2O_5 thin films deposited by the spray pyrolysis method and reported a similar orthorhombic structure [26]. The obtained high intense peak at 35.5^o corresponds to plane values (201) respectively. The average crystallite size can be calculated from the Debye Scherrer equation [27-28].

$$D = \frac{k\lambda}{\beta \cos\theta} \quad (1)$$

where λ is wavelength (1.54 Å), k is Scherrer's constant, β is full width at half maximum (FWHM) of the diffraction spectra, and θ is diffraction angle. Due to the ionic radius of V_2O_5, the average crystallite size of the thin films decreases from 32 to 26.8 nm with increasing molarities. With an increase in molarity percentage, the minute peaks disappear in comparison to pure V_2O_5. Furthermore, together with V_2O_5 peaks, VO_2 peaks are also observed in the XRD pattern of the undoped film, which may due to high deposition temperature [29]. As molarities increase, the average dislocation density and average microstrain of thin films are linearly increased.

3.2. SEM with EDAX

Surface morphology of prepared V_2O_5 thin films with different molar concentrations (2 & 4%) coated on ITO substrate. All the micrographs are taken at different magnifications. Figure 3 (a-c) shows the stacked layers of V_2O_5 with a brick-like arrangement with the whole agglomeration of the particles undefined in the pure V_2O_5 thin film. But under 2 percent of

Table 4: Electrical parameters of pure and ITO (2 and 4%) coated V_2O_5 thin films

Sample	Resistivity (ρ)(Ω cm)	Conductivity (σ)(Ω cm)$^{-1}$	Mobility (μ)(cm^2/Vs)
Pure	2.1x10^{-3}	4.61x10^2	2 x10^1
2%	6.81x10^{-4}	1.42x10^3	4.24x10^1
4%	2.08x10^{-3}	4.75x10^2	3.9 x10^1

molarity, the thin film shows rough morphology with uniform aggregated grain structure. On further increases in molar percentage, the material forms crumbled paper-like morphology in the sheet-like layer arrangement. The increased molar concentration forms a smooth arrangement on comparing the obtained results of 4 % and can be utilized for further characterization and application. However, at 2% molarity, the crystal grain boundaries become blurred again, indicating crystal dissolution. As a result, it was proposed that the optimum molarity for better crystal quality of V_2O_5 films is between 2 and 4%. Increased molarity may result in significant loss of oxygen concentration as well as several key elements of the film, deteriorating the crystal structure. High molarity, in fact, increases the rapid diffusion of V_2O_5 into the substrate layers, which can easily modify the characteristics of the transparent electrode. The presence of significant amounts of vanadium and oxygen on the deposited film was confirmed by elemental composition analysis of the film using EDAX in 2% molarity of ITO coated V_2O_5 thin film (Fig 3d). According to EDAX analysis, no further impurity contamination was discovered on the film.

3.2.1. Surface Occupancy plots

Figure 4 (a-c) depicts Surface Occupancy Plots (SOP) of thin films. Using Image J software, the surface occupancy plot of the deposited thin films was plotted. Furthermore, the agglomeration was increased as traced in Fig 4(b) as a result of the increased particle accumulation density, as evidenced by scanned SEM images. The interactive 3D image as seen in Fig 4 (c) had sheet-like particles uniformly distributed over the scanning surface area.

3.3. Functional group analysis

Figure 5 shows the FT-IR spectrum of pure V_2O_5 produced at two different mole percentages (2% and 4%). The absorption of IR in molecular vibrations further confirms the presence of functional groups in thin films. A vibrational frequency of 421 cm^{-1} represents the stretching vibration of the metal-oxygen link [30-31]. The strong, intense peak at 3199 cm-1 is caused by water molecules stretching vibration O-H bonds [32]. An initial precursor contained nitrate ions, as evidenced by the peak at, 1412 cm^{-1} caused by nitrate stretching vibration (NO^{3-}) [33].

3.4. UV-Visible analysis

A UV-Vis spectrum of samples of pure V_2O_5 at two different molarities is shown in Fig 6, and a band gap calculation is shown in Fig 7. As the molarity rises, the absorbance falls. Transmittance drops abruptly between 300 nm and 800 nm due to absorption of most incoming photons. The Fig 6 shows the region of fundamental absorption edge for ITO coated V_2O_5 thin films with absorbance values of 364.8, 361.3, and 360.5 at pure, 2% and 4% molarities. As crystalline size decreases, the absorption edge shows a red shift in wavelength, which indicates a shift on the lower energy side [34-35]. ITO-coated V_2O_5 thin films with different molarities have different optical properties depending on their microstructure and growth conditions.

The optical band gap energies are 2.18, 2.42 and 2.89 eV for pure and ITO coated V_2O_5 thin films at different molarity, respectively. According to the Brus equation [36], the band gap energies increase with increasing molarities. As a result of quantum size effects [37], the bandgap widening in V_2O_5 thin films is even greater at low growth temperatures, where grain sizes are relatively small ($\leq$50 nm). Moreover, the mean crystal dimension decreases, resulting in a smaller band gap due to quantum size effects [38]. A vacancy in the lattice of V_2O_5 thin films creates lower absorption bands in the optical spectrum due to oxygen vacancies between two V-O layers. The disordered atomic arrangement causes this oxygen vacancy.

3.5. Electrical Studies

At room temperature, the Hall-effect was used to measure the transport parameters. Fig. 8 depicts the alteration of electrical transport characteristics as a function of films. Vanadium ions exhibit various semiconducting properties as a result of their various oxidation states, which is explained by the process of a 3d unpaired electron hopping from a V^{4+} to a V^{5+} ion. It is evident from Fig. 8 that the thin film's conductivity rises as a result of the creation of O vacancies, which is what is referred to as a low mobility n-type semiconductor. Doping has a significant impact on the material's mobility overall. The mixed-phase of V_2O_5 may be the cause of the low electrical conductivity of the undoped film in this instance. For 2% of the molar concentration, the resistivity and mobility of the thin films increase gradually and then decrease for 4% of the molar concentration, while the conductivity values are inversely proportional to the resistivity phenomenon, i.e., it decreases (for 2% of molar concentration) and then increases (for 4% of molar concentration).

4. Conclusion

Spray pyrolysis method was successfully used to prepare V_2O_5 and ITO coated V_2O_5 nanoparticles. The XRD pattern depicts the peaks of the orthorhombic V_2O_5 thin films that were prepared. The average crystallite size of Pure V_2O_5, doped with 2 and 4% molarities, is 32, 29 and 26 nm, respectively. The size of the crystallites reduces as the molar percentages

increase. The FT-IR spectra display the proper bond bands found in the processed materials. While the optical spectra show their corresponding absorption spectra with their respective band gaps, indicating that the produced material is a semiconductor indirectly. Furthermore, with 4% molar concentration, the SEM/EDAX micrographs show that the synthesised thin films were formed in the shape of crumbled paper. Surface occupancy plots, on the other hand, reveal that sheet-like particles are consistently dispersed across the scanning surface area. As a result, the current work reveals that increasing the percent of molarities in V_2O_5 thin-films created using spray pyrolysis improves their optical and electrical properties, allowing the prepared samples to be used for useful optical and electrical applications.

References

[1] G. Kamarajan, D. Benny Anburaj, V. Porkalai, A. Muthuvel & G. Nedunchezhian, "Effect of temperature on optical, structural, morphological and antibacterial properties of biosynthesized ZnO nanoparticles", Journal of the Nigerian Society of Physical Sciences **4** (2022) 892. https://doi.org/10.46481/jnsps.2022.892

[2] M. Arunachalam, P. Thamilmaran & K. Sakthipandi, "Tunning of metal-insulator phase transition temperature in $La_{0.3}Ca_{0.7}MnO_3$ perovskite material", Materials Letters **218** (2018) 270. https://doi.org/10.1016/j.matlet.2018.02.032.

[3] P. Thamilmaran, M. Arunachalam, S. Sankarrajan, K. Sakthipandi, E. J. J. Samuel & M. Sivabharathy, Study of the effect of Cu doping in $La_{0.7}Sr_{0.3}MnO_3$ perovskite materials employing on-line ultrasonic measurements, Journal of Magnetism and Magnetic Materials **443** (2017) 29. https://doi.org/10.1016/j.jmmm.2017.07.046.

[4] R. Rajesh Kanna & K. Sakthipandi, "Structural, Morphological & Optomagnetic Properties of La/Cu/Cu-Mn Ferrite Ternary Nanocomposites", Journal of Electronic Materials **49** (2019) 1110. https://doi.org/10.1007/s11664-019-07729-y.

[5] K. Adavallan, K. Gurushankar, S.S. Nazeer, M. Gohulkumar, R. S. Jayasree & N. Krishnakumar, "Optical redox ratio using endogenous fluorescence to assess the metabolic changes associated with treatment response of bioconjugated gold nanoparticles in streptozotocin-induced diabetic rats", Laser Physics Letters **14** (2017) 065901. https://doi.org/10.1088/1612-202X/aa6b21

[6] A. Ezra, Z. Shehu, W. L. Danbature, K. P. Yoriyo, R. D. Kambel & C. N. Ayuk, "A Novel development of ZnO/SiO2 nanocomposite: a nanotechnological approach towards insect vector control", Journal of the Nigerian Society of Physical Sciences **3** (2021) 262. https://doi.org/10.46481/jnsps.2021.198.

[7] V. Balasundaram, V. Balasubramanian, T. Senthil Siva Subramanian, J. Henry, T. Daniel, K. Mohanraj and G. Sivakumar, Effect of adding Ce on the optostructural and electrical properties of cubic CaSnO3. Phosphorus, Sulfur, and Silicon and the Related Elements **197** (2022) 176. doi.org/10.1080/10426507.2021.2014487

[8] G. R. Mutta, S. R. Popuri, M. Maciejczyk, N. Robertson & M. Vasundhara, "V_2O_5 as an inexpensive counter electrode for dye snesitized solar cells", Materials Research Express **3** (2016) 1. https://doi.org/10.1088/2053-1591/3/3/0355.

[9] J. M. Lee, H.S. Hwang, W. II Cho, B.W. Cho, K.Y. Kim, "Effect of silver co-sputtering on amorphous V_2O_5 thin –films for micro batteries", Journal Power sources **136** (2004) 122. doi: 10.1016/j.jpowsour.2004.05.051

[10] K. Sieradzka, D. Wojcieszak, D. Kaczmarek, J. Domaradzki, G. Kiriakidis, E. Aperathitis & S. Song, "Structural and optical properties of vanadium oxides prepared by microwave-assisted reactive magnetron sputtering", Optica Application **41** (2011) 463.

[11] Q. H. Wu, A. Thissen, W. Jaegermann, & M. Liu, "Photoelectron spectroscopy study of oxygen vacancy on vanadium oxides surface", Applied Surface Science **236** (2004) 473. https://doi:10.1016/j.apsusc.2004.05.112.

[12] A. J.Santos, B. Lacroix, M. Domínguez, R.García, N. Martin & F. M. Morales, Controlled grain-size thermochromic VO_2 coatings by the fast oxidation of sputtered vanadium or vanadium oxide films deposited at glancing angles, surface and interface **27** (2021) 101581, doi: 10.1016/j.surfin.2021.101581

[13] Xun Cao, Tianci Chang, Zewei Shao, Fang Xu, Hongjie Luo, Ping Jin, Challenges and Opportunities toward Real Application of VO_2-Based Smart Glazing, Matter **2** (2020) 832.

[14] Di Wu, Qianqian Su, Yang Li, Chen Zhang, Xian Qin, Yuan-Yuan Liu, Wen-Song Xi, Yanfeng Gao, Aoneng Cao, Xiaogang Liu, Haifang Wang, Toxicity assessment and mechanistic investigation of engineered monoclinic VO 2 nanoparticles, Nanoscale **24** (2018) 9736. doi: 10.1039/c8nr02224k.

[15] H. Wu, M. Li, L. Zhong, Y. Y. Luo, G. H. Li, "Electrochemical Synthesis of Amorphous VO_2 Colloids and Their Rapid Thermal Transforming to VO_2(M) Nanoparticles with Good Thermochromic Performance", Chemistry A European Journal (2016). https://doi.org/10.1002/chem.201604101

[16] M. M. Sajid, N. A. Shad, Y. Javed, S. BashirKhan, Z. Zhang, N. Amin, H. Zhai, "Preparation and characterization of Vanadium pentoxide (V_2O_5) for photocatalytic degradation of monoazo and diazo dyes", Surface and Interface **19** (2020) 100502. https://doi.org/10.1016/j.surfin.2020.100502

[17] A. EEl Haimeur, A. Mrigal, H. Bakkali, L. El Gana, K. Nouneh, M. Addou & M. Dominguez, "Optical, magnetic, and electronic properties of nanostructured VO2 thin films grown by spray pyrolysis: DFT first principle study", Journal of Superconductivity and Novel Magnetism **33** (2020) 511. https://doi.org/10.1007/s10948-019-05216-3

[18] R. Berenguer, Ma. O. Guerrero-Pérez, I. Guzmán, J. Rodríguez-Mirasol & T. Cordero, "Synthesis of Vanadium Oxide Nanofibers with Variable Crystallinity and V^{5+}/V^{4+} Ratios", ACS Omega **2** (2017) 7739. https://doi.org/10.1021/acsomega.7b01061

[19] S. K. Park, P. Nakhanivej, J. S. Yeon, K. H. Shin, W. M. Dose, M. De Volder, J. B. Lee, H. J. Kim & H. S. Park, "Electrochemical and structural evolution of structured V2O5 microspheres during Li-ion intercalation", journal of energy chemistry **55** (2021) 108. doi.org/10.1016/j.jechem.2020.06.028

[20] Y. Ge, X. Xie, J. Roscher, *et al.*, "How to measure and report the capacity of electrochemical double layers, supercapacitors, and their electrode materials", Journal of solid-State electrochemistry **24** (2020) 3215. doi.org/10.1007/s10008-020-04804-x

[21] S. Deng, Z. Yuan, Z. Tie, C. Wang, L. Song, and Z. Niu, Electrochemically Induced Metal–Organic-Framework-Derived Amorphous V_2O_5 for Superior Rate Aqueous Zinc-Ion Batteries. Angewandte Chemie International Edition **59** (2020) 22002. doi.org/10.1002/anie.202010287

[22] K. Karthik, M. P. Nikolova, A. Phuruangrat, S. Pushpa, V. Revathi & M. Subbulakshmi, "Ultrasound-assisted synthesis of V2O5 nanoparticles for photocatalytic and antibacterial studies", Materials Research Innovations **24** (2020) 229. doi.org/10.1080/14328917.2019.1634404

[23] M. Rafique, M. Hamza, M. B. Tahir, S. Muhammad & A. G. Al-Sehemi, "Facile hydrothermal synthesis of highly efficient and visible light-driven Ni-doped V2O5 photocatalyst for degradation of Rhodamine B dye", Journal of Materials Science: Materials in Electronics **31** (2020) 12913. doi.org/10.1007/s10854-020-03844-3

[24] M. Benmoussa, A. Outzourhit, A. Bennouna & E. L. Ameziane, "Electrochromism in sputtered V2O5 thin films: structural and optical studies", Thin Solid Films, 405 (2002) 11. doi.org/10.1016/S0040-6090(01)01734-5

[25] G. T. Mola, E.A. Arbab, B. A. Taleatu, K. Kaviyarasu, I. Ahmad and M. Maaza, "Growth and characterization of V_2O_5 thin film on conductive electrode. Journal of Microscopy" 265 (2017) 214. doi.org/10.1111/jmi.12490

[26] R. Rathika, M. Kovendhan, D. Paul Joseph, Rekha Pachaiappan, A. Sendil Kumar, K. Vijayarangamuthu, C. Venkateswaran, K. Asokan, S. J. Jeyakumar, "Tailoring the properties of spray deposited V2O5 thin films using swift heavy ion beam irradiation", Nuclear Engineering and Technology **52** (2020) 2585. doi.org/10.1016/j.net.2020.04.013

[27] E. Ahilandeswari, R. R. Kanna & K. Sakthipandi, "Synthesis of neodymium-doped barium nanoferrite: analysis of structural, optical, morphological, and magnetic properties", Physica B: Condensed Matter **599** (2020) 412425. doi.org/10.1016/j.physb.2020.412425

[28] R. R. Kanna, K. Sakthipandi, A.S. Kumar, N.R Dhineshbabu,

S.M. seeni Mohamed Aliar Maraikkayar, A.S. Afroze, R.B. Jotania and M. Sivabharathy, Synthesis of dysprosium/Mn–Cu ferrite binary nanocomposite: Analysis of structural, morphological, dielectric, and optomagnetic properties. Ceramics International **46** (2020) 13695. doi.org/10.1016/j.ceramint.2020.02.157

[29] A. Kumar, P. Singh, N. Kulkarni, D. Kaur, "Structural and optical Studies of nanocrystalline V_2O_5 thin films", Thin Solid Films **516** (2008) 912. doi.org/10.1016/j.tsf.2007.04.165.

[30] P. Periasamy, T. Krishnakumar, B. Selvakumar, K. Gurushankar, K. Senthilkannan & M. Chavali, "Structural, thermal, optical and dielectric studies of V2O5@ WO3 nanocomposites prepared by microwave-assisted hydrothermal method", Applied Physics A 127 (2021) 1. doi.org/10.1007/s00339-021-05101-8

[31] C. Thangamani, P. Vijaya Kumar, K. Gurushankar & K. Pushpanathan, "Structural and size dependence magnetic properties of Mn-doped NiO nanoparticles prepared by wet chemical method", Journal of Materials Science: Materials in Electronics **31** (2020) 11101. doi.org/10.1007/s10854-020-03659-2

[32] E. Ahilandeswari, K. Sakthipandi, R. R. Kanna, M. Hubálovská & D. Vigneswaran, "Lanthanum substitution effect on the structural, optical, and dielectrical properties of nanocrystalline BaFe2O4 ferrites", Physica B: Condensed Matter **635** (2022) 413849. doi.org/10.1016/j.physb.2022.413849

[33] N. Al-Zaqri, K. Umamakeshvari, V. Mohana, A. Muthuvel and A. Boshaala, "Green synthesis of nickel oxide nanoparticles and its photocatalytic degradation and antibacterial activity", Journal of Materials Science: Materials in Electronics **33** (2022) 11864. doi.org/10.1007/s10854-022-08149-1

[34] M. Elayaraja, I.K. Punithavathy, M. Jothibas, A. Muthuvel & S.J. Jeyakumar, "Effect of rare-earth metal ion Ce3+ on the structural, optical and photocatalytic properties of CdO nanoparticles", Nanotechnology for Environmental Engineering **5** (2020) 1. doi.org/10.1007/s41204-020-00091-z

[35] T. Daniel, K. Mohanraj & G. Sivakumar, "Synthesis and Characterization of $CuMS_2$ (M= Bi, Sb) Thin Films Prepared by CBD Method", Jordan Journal of Physics **11** (2018) 137.

[36] I. K. Punithavathy, A. Rajeshwari, S. Johnson Jeyakumar & L. Nayagam, "Impact of lanthanum ions on magnetic and dielectric properties of cobalt nanoferrites", Journal of Materials Science: Materials in Electronics **31** (2020). https://doi.org/10.1007/s10854-020-03523-3.

[37] A. Muthuvel, M. Jothibas, V. Mohana and C. Manoharan, Green synthesis of cerium oxide nanoparticles using Calotropis procera flower extract and their photocatalytic degradation and antibacterial activity. Inorganic Chemistry Communications **119** (2020) 108086. doi.org/10.1016/j.inoche.2020.108086

[38] R. R. Kanna, Structural, morphological and optomagnetic properties of GO/Nd/Cu-Mn ferrite ternary nanocomposite. Ceramics International **45** (2019) 16138. doi.org/10.1016/j.ceramint.2019.05.132